JOURNAL OF
Materials
CHEMISTRY

Crystal structures and electrical conducting/magnetic properties in 1 : 1 $FeCl_4$ and $FeBr_4$ salts of dimethylthio- and ethylenedithio-(1,3-dithiolylidene)thioxotetrathiafulvalene radical cations

Tsuyoshi Kominami,[a] Takuya Matsumoto,[a] Kazumasa Ueda,[a] Toyonari Sugimoto,*[a] Keizo Murata,[c] Motoo Shiro[c] and Hideo Fujita[d]

[a] *Research Institute for Advanced Science and Technology, Osaka Prefecture University, Sakai, Osaka, 599-8570, Japan. E-mail: toyonari@iwate.riast.osakafu-u.ac.jp*
[b] *Graduate School of Science, Osaka City University, Sumiyoshi, Osaka, 558-8585, Japan*
[c] *Rigaku Corporation, Akishima, Tokyo 196-8666, Japan*
[d] *Department of Natural Environment, Faculty of Integrated Human Studies, Kyoto University, Kyoto 606-8501, Japan*

Received 26th February 2001, Accepted 10th May 2001
First published as an Advance Article on the web 12th June 2001

The 1 : 1 radical cation salts of new donor molecules, dimethylthio- (**1**) and ethylenedithio-(1,3-dithiolylidene)thioxotetrathiafulvalenes (**2**) with a magnetic $FeCl_4$ or $FeBr_4$ counteranion (**1**·$FeBr_4$, **2**·$FeCl_4$ and **2**·$FeBr_4$) were prepared, and their electrical conducting and magnetic properties were investigated. The room-temperature electrical conductivities of **1**·$FeBr_4$ (compressed pellet), **2**·$FeCl_4$ (single crystal) and **2**·$FeBr_4$ (single crystal) were $<10^{-5}$, 1.8×10^{-4} and 7.0×10^{-2} S cm^{-1}, respectively. The temperature dependence of paramagnetic susceptibility obeyed the Curie–Weiss law in all cases, and the Curie constant (C) and Weiss temperature (θ) were as follows: $C = 4.61$ emu K mol^{-1} and $\theta = -5.4$ K for **1**·$FeBr_4$; $C = 4.53$ emu K mol^{-1} and $\theta = -13.4$ K for **2**·$FeCl_4$; $C = 4.55$ emu K mol^{-1} and $\theta = -31.2$ K for **2**·$FeBr_4$. The remarkably different θ values between the three salts, considered together with their crystal structures, suggest significant interaction between Fe(III) spins by aid of π spins on **1** or **2** molecules.

Introduction

Now that a number of molecular conductors and superconductors have been discovered mostly based on charge-transfer salts of organo-chalcogenide donors with a variety of non-magnetic inorganic or organic counteranions, current interest is intensively directed toward molecular magnetic conductors and superconductors, in which conductivity or superconductivity coexists with magnetism regardless of interplay between them.[1] In particular, it is an ultimate target to develop molecular ferromagnetic metallic and super-conductors. Since the start of this kind of investigation in around 1985, there has already been some achievement of a paramagnetic superconductor,[2] an antiferromagnetic superconductor[3] and a ferromagnetic metallic conductor[4] in molecular/organic solids. Nevertheless, the number is too few to understand more fully the electronic and magnetic properties in molecular magnetic conductors, so that new donor molecules are needed for the preparation of further charge-transfer salts with several magnetic counteranions. New donor molecules we very recently prepared, dimethylthio- (**1**) and ethylenedithio-(1,3-dithiolylidene)thioxotetrathiafulvalenes† (**2**) can be expected as reliable candidates for the development of molecular magnetic conductors,[5] since significant interaction between conducting π electrons on **1** or **2** molecules and local d spins on the Cu(II) ions was recognized in their complexes with $CuBr_2$[6] and in their charge-transfer salts with a $CuCl_4$ or $CuBr_4$ counter-anion.[7] Unfortunately, metallic or super-conductivity and/or ferromagnetism which was our aim was not achieved at all by any of the Cu complex and charge-transfer salts. Subsequently efforts were made for the preparation of charge-transfer salts of **1** and **2** with a magnetic FeX_4 (X = Cl, Br) counteranion, since the FeX_4 ion is monoanionic like non-magnetic inorganic anions (ClO_4, BF_4, PF_6, AsF_6, SbF_6, I_3 *etc.*) for metallic and super-conducting charge-transfer salts of organo-chalcogenide donors. The present paper reports on the crystal structures, and electrical conducting and magnetic properties of the $FeCl_4$ and $FeBr_4$ salts. The $FeCl_4$ and $FeBr_4$ salts of some donor molecules, bis(ethylenedithio)tetrathiafulvalene (BEDT-TTF),[8,9] bis(methylthio)ethylenedithiotetrathiafulvalene (C_1TET-TTF),[10,11] 4,5-ethylenedithio-4′,5′-dimethyl-1,3-dithia-1′,3′-diselenafulvalene (DMET)[12] and bis(ethylenedithio)tetraselenafulvalene (BETS)[3,13] are so far known, of which metallic and super-conductivities were observed for $(DMET)_2{\cdot}FeBr_4$[12] and $(BETS)_2{\cdot}FeBr_4$[3] respectively. Furthermore, strong spin interaction between the Fe(III) ($S = 5/2$) spins also occurred for $(BETS)_2{\cdot}FeBr_4$.[3]

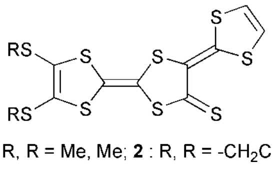

1 : R, R = Me, Me; **2** : R, R = $-CH_2CH_2-$

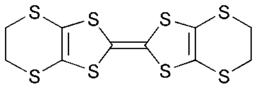

BEDT-TTF

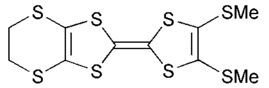

C_1TET-TTF

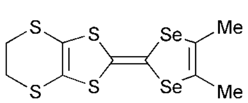

DMET

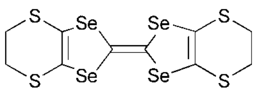

BETS

---

†These compounds were previously named as dimethylthio- and ethylenedithio-tetrathiafulvalenothioquinone-1,3-dithiolemethides.

DOI: 10.1039/b101547h

Experimental

Synthesis of **1**·$FeBr_4$, **2**·$FeCl_4$ and **2**·$FeBr_4$

A CS_2 solution (0.5 ml) of **1** or **2** (1.2×10^{-3} mmol) was in contact with a CH_3CN solution (0.6 ml) of $FeCl_3$ or $FeBr_3$ (4.5×10^{-2} mmol) at 20 °C for one week. At the interface between the two solutions black crystals of **1**·$FeBr_4$ (mp > 300 °C), **2**·$FeCl_4$ (mp > 300 °C) and **2**·$FeBr_4$ (mp > 300 °C) were precipitated. No crystal was obtained by the reaction of **1** with $FeCl_3$. Anal. Calcd. for $C_{11}H_8S_9Fe_1Br_4$ (**1**·$FeBr_4$): C, 16.43; H, 1.00; N, 0%. Found: C, 16.34; H, 1.07; N, 0%. Anal. Calcd. for $C_{11}H_6S_9Fe_1Cl_4$ (**2**·$FeCl_4$): C, 21.16; H, 0.97; N, 0%. Found: C, 21.36; H, 1.18; N, 0%. Anal. Calcd. for $C_{11}H_6S_9Fe_1Br_4$ (**2**·$FeBr_4$): C, 16.47; H, 0.75; N, 0%. Found: C, 16.56; H, 0.65; N, 0%.

X-Ray data collection, structure solution, and refinement

Intensity data of **1**·$FeBr_4$, **2**·$FeCl_4$ and **2**·$FeBr_4$ were measured on a Rigaku RAXIS-RAPID imaging plate diffractometer using graphite monochromated MoKα radiation ($\lambda = 0.71069$ Å). Experimental details and crystal data are given in Table 1. The structures were solved by direct methods (SIR92[14] and DIRDIF94[15]), and refined on F_o^2 with full-matrix least-squares analysis. Calculated positions of the hydrogen atoms [d(C–H) = 0.95 Å] were included in the final calculation. All the calculations were performed by using the teXsan crystallographic software package of the Molecular Structure Corporation.[16] For **1**·$FeBr_4$ the final cycle of least-squares refinement on F_o^2 for 4848 data and 198 parameters converged to $wR2(F_o^2) = 0.214$ for all data and to $R1 = 0.081$ for 2339 data with $I \geqslant 3\sigma(I)$. For **2**·$FeCl_4$ the final cycle of least-squares refinement of F_o^2 for 4618 data and 226 parameters converged to $wR2(F_o^2) = 0.103$ for all data and to $R1 = 0.056$ for 2851 data with $I \geqslant 1\sigma(I)$. For **2**·$FeBr_4$ final cycle of least-squares refinement of F_o^2 for 4789 data and 226 parameters converged to $wR2(F_o^2) = 0.127$ for all data and to $R1 = 0.066$ for 2536 data with $I \geqslant 1\sigma(I)$.

Electrical conductivity, magnetic susceptibility, and EPR measurements

Electrical conductivity was measured on the compressed pellet or single crystal of the $FeCl_4$ or $FeBr_4$ salt using a two- or four-probe method at room temperature. For **2**·$FeBr_4$ the temperature dependence of electrical conductivity was also investigated in the temperature range of 80–300 K. The contact to the electrode was performed with gold paste. The magnetic susceptibility (χ_{obs}) of the microcrystals was measured between 5 and 300 K at an applied field of 1 kOe using a SQUID magnetometer (MPMS XL, Quantum Design). The paramagnetic susceptibility (χ_p) was obtained by subtracting the diamagnetic contribution calculated by a Pascal method[17] from χ_{obs}. The EPR spectrum of the microcrystals was recorded using a JEOL 1X spectrometer. For determining the g value, a sample of $MnSO_4 \cdot H_2O$ diluted with MgO was used as a reference.

Table 1 Crystallographic data for **1**·$FeBr_4$, **2**·$FeCl_4$ and **2**·$FeBr_4$

	1·$FeBr_4$	**2**·$FeCl_4$	**2**·$FeBr_4$
Temperature/K	113	298	298
Empirical formula	$C_{11}H_8S_9Br_4Fe$	$C_{11}H_6S_9Cl_4Fe$	$C_{11}H_6S_9Br_4Fe$
MW	804.19	624.37	802.17
Crystal system	Triclinic	Monoclinic	M onoclinic
Space group	$P\bar{1}$	$P2_1/c$	$P2_1/c$
a/Å	8.6768(7)	15.222(3)	15.464(1)
b/Å	10.5170(3)	7.4915(9)	7.4292(4)
c/Å	14.2544(9)	18.537(3)	19.085(1)
α/°	69.509(7)		
β/°	76.406(3)	91.874(6)	92.438(5)
γ/°	83.126(3)		
V/Å^3	1183.3(1)	2112.8(6)	2190.6(3)
d_{calcd}/g cm^{-3}	2.257	1.963	2.432
Z	2	4	4
μ/cm^{-1}	82.01	21.04	88.61
Total reflns.	8249	18415	18402
No. of obsd. reflns.	2339	2851	2536
$R1^a$	0.081	0.056	0.066
$WR2^b$	0.214	0.103	0.127
GOF^c	1.91	1.02	1.03

$^a R1 = (\Sigma||F_o| - |F_c||)/(\Sigma|F_o|)$. $^b wR2 = [\Sigma w(F_o^2 - F_c^2)^2/\Sigma w(F_o^2)^2]^{1/2}$. $^c \mathrm{GOF} = \{\Sigma[w(F_o^2 - F_c^2)^2]/(n-p)\}^{1/2}$.

Results and discussion

Crystal structures of **1**·$FeBr_4$, **2**·$FeCl_4$ and **2**·$FeBr_4$‡

As seen from the projections down to ab and [101] planes in Fig. 1a,b, the **1** molecules in **1**·$FeBr_4$ are stacked along the c axis to form a one-dimensional column, all of which are arranged in a parallel fashion. However, the column is composed of dimerized **1** molecules with an effective overlap and a shorter interplanar distance (3.35 Å) than 'a π-cloud thickness' (3.40 Å) (see Fig. 1c).[18] On the other hand, the interdimer has an inferior overlap and a longer interplanar distance (3.52 Å) than the intradimer (also see Fig. 1c). Each $FeBr_4$ ion has a slightly distorted tetrahedral geometry of four Br atoms around the central Fe atom, as is obvious from the six Br–Fe–Br bond angles (107.1(3), 109.1(3), 109.4(3), 109.8(3), 110.4(3), 111.0(3)°). The $FeBr_4$ ions are located near the intradimers and also arranged along the c axis. The two arrays of $FeBr_4$ ions face each other between the neighboring **1** columns. The shortest contact distance between one S atom of the 1,3-dithiole group in the **1** molecule and one Br atom in the $FeBr_4$ ion is 3.60 Å, which is comparable to the sum of the van der Waals radii of S and Br atoms (3.65 Å).[18] The Br···Br contact distances within an $FeBr_4$ ion array and between the neighboring $FeBr_4$ ion arrays are 5.11 and 4.50 Å, respectively, which are much longer than a normal van der Waals contact between two Br atoms (3.80 Å).[18]

On the other hand, the crystal structures of **2**·$FeCl_4$ and **2**·$FeBr_4$ are shown in Fig. 2a,b and Fig. 3a,b, respectively, which are projections down to the ac and bc planes. On the whole, their stacking structures are similar to that of **1**·$FeBr_4$. However, there is a large difference in the mutual arrangement between the columns of **1** and **2** molecules. Thus, as mentioned above, all the **1** columns are arranged in a parallel fashion, while the **2** columns are alternately tilted from each other by 44.0(8) and 42.8(4)° for **2**·$FeCl_4$ and **2**·$FeBr_4$, respectively. This different mutual arrangement between the **1** and **2** columns also exerted a significant influence on the arrangement of $FeCl_4$ or $FeBr_4$ ions. The stacking structures of the **2** molecules in **2**·$FeCl_4$ and **2**·$FeBr_4$ are very similar to each other, as shown in Fig. 2c and Fig. 3c. The interplanar distances of the intradimers are 3.34 and 3.36 Å for **2**·$FeCl_4$ and **2**·$FeBr_4$ respectively, and the interdimers have the same interplanar distance of 3.68 Å. Also in these cases, the geometry of $FeCl_4$ and $FeBr_4$ ions is slightly distorted tetrahedral: the Cl–Fe–Cl bond angles are 107.5(1), 107.5(1), 108.8(1), 109.9(1), 110.4(1) and 112.8(1)° for the $FeCl_4$ ion, and the Br–Fe–Br bond angles are 107.7(1), 108.0(1), 109.0(1), 109.5(1), 110.7(1) and 111.9(1)° for the $FeBr_4$ ion. Both $FeCl_4$ and $FeBr_4$ ions are also near the intradimers, and very close contacts are present between one S atom of the 1,3-dithiole group in the **2** molecule and one Cl or Br atom in the $FeCl_4$ or $FeBr_4$ ion. The S···Cl and S···Br distances are 3.23 and 3.38 Å, respectively, which are remarkably short as compared with those (3.55 and 3.65 Å)

---

‡CCDC reference numbers 162728–162730. See http://www.rsc.org/suppdata/jm/b1/b101547h/ for crystallographic files in .cif format.

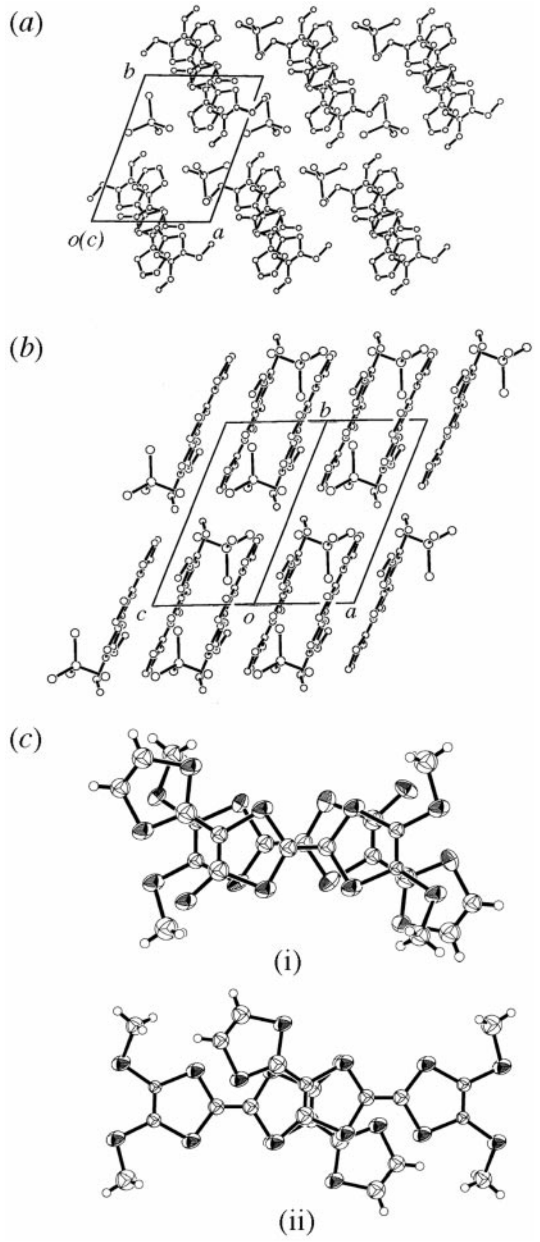

Fig. 1 Crystal structure of **1**·$FeBr_4$: (*a*) projection down to the *ab* plane, (*b*) projection down to the [101] plane, and (*c*) (i) intradimer and (ii) interdimer stacking structures of **1** molecules.

of the corresponding van der Waals contacts.[18] Within an $FeCl_4$ or $FeBr_4$ ion array the neighboring ions are very remote from each other, as is seen from much larger Cl···Cl (4.82 Å) and Br···Br contact distances (4.64 Å) than those (3.67 and 3.80 Å) of the corresponding van der Waals contacts.[18] Shorter Cl···Cl and Br···Br contacts rather occur between the neighboring $FeCl_4$ or $FeBr_4$ ion arrays. Their contact distances are 3.68 and 3.79 Å, respectively, which are almost comparable to those of the corresponding van der Waals contacts.

Electrical conductivities

The electrical conductivity measurement was performed on a compressed pellet for **1**·$FeBr_4$, whose crystal size was too small to be contacted to the electrode, but on single crystals for **2**·$FeCl_4$ and **2**·$FeBr_4$. The values at room temperature were $<10^{-5}$, 1.8×10^{-4} and 7.0×10^{-2} S cm^{-1}, respectively, which are actually low, but higher as compared with those of 1 : 1 $FeCl_4$ or $FeBr_4$ salts of BEDT-TTF and C_1TET-TTF prepared so far: *ca.* 10^{-6}, 2×10^{-7} and 2×10^{-7} S cm^{-1} for (BEDT-TTF)·$FeBr_4$,[8] (C_1TET-TTF)·$FeCl_4$[10,11] and (C_1TET-TTF)·$FeBr_4$,[10,11] respectively. In particular, the high electrical conductivity of **2**·$FeBr_4$ is remarkable; its temperature dependence however exhibited semiconducting behavior with a fairly large activation energy of 0.15 eV. The low electrical conductivities of the present salts are on the whole due to 1 : 1 stoichiometry of the **1** or **2** molecule and $FeCl_4$ or $FeBr_4$ ion, and also strong dimerization of the donor molecules, although the contact between the neighboring interdimers is much better for **2**·$FeCl_4$ and **2**·$FeBr_4$ than for **1**·$FeBr_4$, which is proposed as a main cause for the higher observed electrical conductivity for the former salts.

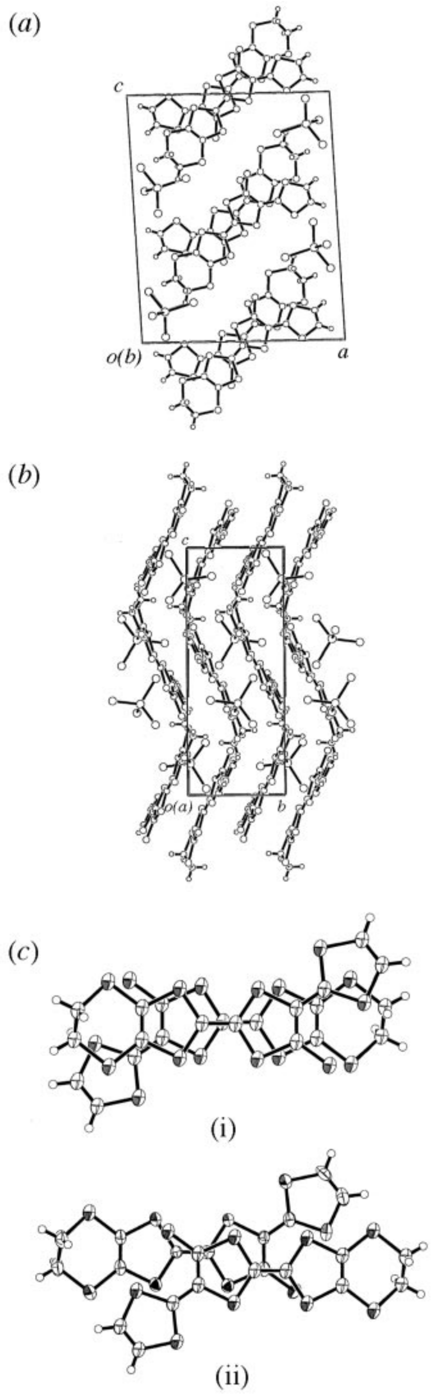

Fig. 2 Crystal structure of **2**·$FeCl_4$: (*a*) projection down to the *ac* plane, (*b*) projection down to the *bc* plane, and (*c*) (i) intradimer and (ii) interdimer stacking structures of **2** molecules.

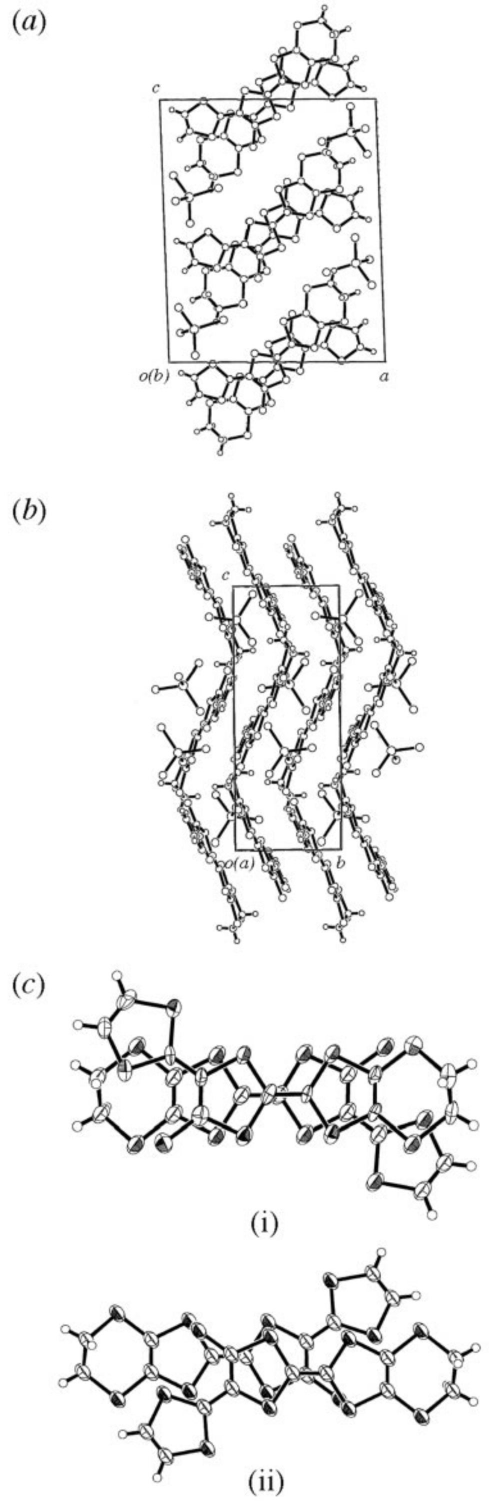

Fig. 3 Crystal structure of **2**·$FeBr_4$: (*a*) projection down to the *ac* plane, (*b*) projection down to the *bc* plane, and (*c*) (i) intradimer and (ii) interdimer stacking structures of **2** molecules.

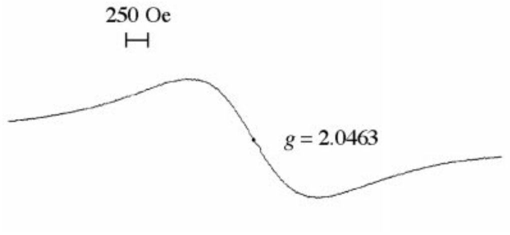

Fig. 4 Room-temperature EPR spectrum of microcrystals of **2**·$FeBr_4$.

EPR

The room-temperature EPR spectra of the microcrystals of **1**·$FeBr_4$ and **2**·$FeBr_4$ showed very broad doublet signals ($\Delta H_{pp} = 1403$ and 1333 Oe) at $g = 2.0485$ and 2.0463, respectively. Also in the EPR spectrum of the microcrystals of **2**·$FeCl_4$ at room temperature, only one broad signal ($\Delta H_{pp} = 156$ Oe) was observed at $g = 2.0214$. A typical EPR spectrum of **2**·$FeBr_4$ is shown in Fig. 4. No signal due to the π spin on the radical cations of **1** and **2** ($\mathbf{1}^{+\bullet}$ and $\mathbf{2}^{+\bullet}$) appeared in any of the spectra, suggesting a possibility of either strong dimerization of the $\mathbf{1}^{+\bullet}$ or $\mathbf{2}^{+\bullet}$ molecules or significant interaction between the Fe(III) d spin and the $\mathbf{1}^{+\bullet}$ or $\mathbf{2}^{+\bullet}$ π spin. In order to determine which spin interaction actually occurs in these $FeCl_4$ and $FeBr_4$ salts, Et_4N·$FeCl_4$ and Et_4N·$FeBr_4$ were measured as reference compounds of $FeCl_4$ and $FeBr_4$ salts with no π spins, and their *g* and ΔH_{pp} values (2.0226 and 158 Oe for Et_4N·$FeCl_4$, and 2.0503 and 568 Oe for Et_4N·$FeBr_4$) were compared to those of the present $FeCl_4$ and $FeBr_4$ salts. All the *g* values of **2**·$FeCl_4$, **1**·$FeBr_4$ and **2**·$FeBr_4$ are definitely smaller than those of the corresponding Et_4N·$FeCl_4$ and Et_4N·$FeBr_4$, suggesting significant interaction of the Fe(III) d spin on the $FeCl_4$ or $FeBr_4$ ion with the π spin on the $\mathbf{1}^{+\bullet}$ or $\mathbf{2}^{+\bullet}$ molecule. Assuming that strong interaction occurs between both spins, the observed *g* value can be obtained from the equation $g_{obs} = \chi_{Fe}g_{Fe}/\chi_{total} + \chi_{\pi}g_{\pi}/\chi_{total}$ and $\chi_{total} = \chi_{Fe} + \chi_{\pi}$, where g_{Fe} and g_{π}, and χ_{Fe} and χ_{π} are the *g* values and local magnetic susceptibilities contributed from the individual Fe(III) d spin and $\mathbf{1}^{+\bullet}$ or $\mathbf{2}^{+\bullet}$ π spin, respectively, and χ_{total} the total magnetic susceptibility. The g_{π} values of the BF_4^- salts of $\mathbf{1}^{+\bullet}$ and $\mathbf{2}^{+\bullet}$ are on average 2.0070,[19] so that the g_{obs} values are calculated to be 2.0214 for the **2**·$FeCl_4$ salt, and 2.0469 for **1**·$FeBr_4$ and **2**·$FeBr_4$. Good coincidence between the observed and calculated *g* values is obtained for **2**·$FeCl_4$ and **2**·$FeBr_4$, suggesting that strong interaction indeed occurs between the Fe(III) d spin on the $FeCl_4$ or $FeBr_4$ ion and the π spin on the $\mathbf{2}^{+\bullet}$ molecules. In contrast to these salts, it is obvious for **1**·$FeBr_4$ that the observed *g* value (2.0485) is significantly larger than the calculated one (2.0469). This discrepancy can be readily understood by considering the weak interaction between the Fe(III) d and $\mathbf{1}^{+\bullet}$ π spins. The different π–d spin interaction between **2**·$FeCl_4$ ($FeBr_4$) and **1**·$FeBr_4$ is strongly related to the different S···Cl or S···Br distance between the S atom of the 1,3-dithiole group in the **1** or **2** molecule and the Cl or Br atom in $FeCl_4$ or $FeBr_4$ ion. Thus, for **2**·$FeCl_4$ and **2**·$FeBr_4$ the S···Cl (3.23 Å) and S···Br distances (3.38 Å) are remarkably shorter than the van der Waals contacts between S and Cl or Br atoms (3.55 and 3.65 Å), while **1**·$FeBr_4$ has an S···Br distance (3.60 Å) comparable to the corresponding van der Waals contact.

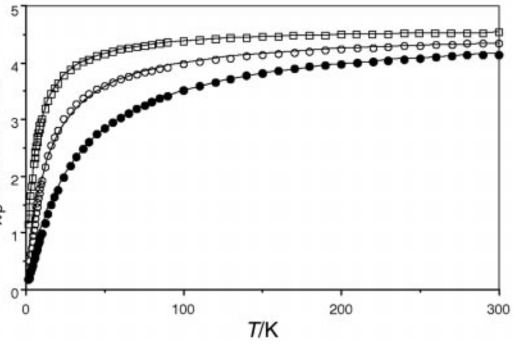

Fig. 5 Temperature dependences of $\chi_p T$ in the temperature range 5 to 300 K for (□) **1**·$FeBr_4$, (○) **2**·$FeCl_4$ and (●) **2**·$FeBr_4$.

Magnetic susceptibilities

Fig. 5 shows the temperature dependences of the product of χ_p with T ($\chi_p T$) between 2 and 300 K for **1**·FeBr$_4$, **2**·FeCl$_4$ and **2**·FeBr$_4$. In all the cases the $\chi_p T$ value gradually decreased with lowering temperature. These can be interpreted as a χ_p–T behavior obeying a Curie–Weiss law, $\chi_p = C/(T-\theta)$ where C is the Curie constant and θ the Weiss temperature. Values which best reproduced the experimental results were as follows: C = 4.61 emu K mol^{-1} and $\theta = -5.4$ K for **1**·FeBr$_4$; C = 4.53 emu K mol^{-1} and $\theta = -13.4$ K for **2**·FeCl$_4$; C = 4.55 emu K mol^{-1} and $\theta = -31.2$ K for **2**·FeBr$_4$. The C values obtained are very close to the value (4.63 emu K mol^{-1}) of an Fe(III) (S = 5/2) spin entity. The π spins on the **1** or **2** molecules form a fairly tight singlet, as is obvious from the crystal structures of these salts, so that apparently their magnetic moments are much reduced. The θ values all have a negative sign indicating antiferromagnetic interaction between the spins, but the magnitude is largely different between the three salts. Thus, the magnitude becomes larger in the order of **1**·FeBr$_4$, **2**·FeCl$_4$ and **2**·FeBr$_4$. In particular, it should be noted that the θ value in **2**·FeBr$_4$ is remarkably larger than those in several FeCl$_4$ and FeBr$_4$ salts obtained so far (−16 K for (C$_1$TET-TTF)·FeBr$_4$).[10,11] The different magnitude of spin interaction between the three salts can be reasonably explained using a schematic spin arrangement as shown in Fig. 6. In this Figure, a, b and c denote the distances of Cl (or Br)···S, shorter Cl (or Br)···Cl (or Br) and longer Cl (or Br)···Cl (or Br) contacts, respectively. The preceding section discussed the relationship between a and the magnitude of π–d interaction. As for b, the value in **1**·FeBr$_4$ is 4.50 Å, which is considerably longer than the distance (3.80 Å) of van der Waals Br···Br contact, while **2**·FeCl$_4$ and **2**·FeBr$_4$ have the values of 3.68 and 3.79 Å, respectively, which are almost equal to the distances (3.67 Å in the Cl case) of van der Waals Cl···Cl and Br···Br contacts. On the other hand, all the c values (5.11, 4.82 and 4.64 Å for **1**·FeBr$_4$, **2**·FeCl$_4$ and **2**·FeBr$_4$, respectively) are considerably longer than the distances of van der Waals Cl···Cl and Br···Br contacts, although the difference between the observed and van der Waals contact distances decreases in the order of **1**·FeBr$_4$ (1.31 Å), **2**·FeCl$_4$ (1.15 Å) and **2**·FeBr$_4$ (0.84 Å). Of course, the θ value reflects the magnitude of one-dimensional spin interaction irrespective of being ferromagnetic or antiferromagnetic, which is inversely related to the interspin distance. In the present case the observed θ value is considered as an average of the spin interaction in the Cl (or Br)···S, shorter Cl (or Br)···Cl (or Br) and longer Cl (or Br)···Cl (or Br) contacts, which are related to a, b and c, respectively. However, the interaction of longer Cl (or Br)···Cl (or Br) contact is presumably very weak as compared with the other interaction for the three salts, so that it is most conceivable that one-dimensional spin alignment of ···{Cl(Br)···Cl(Br)···**1(2)**···**1(2)**}$_n$··· predominantly operates in the solids. This model can indeed explain a very small θ value in **1**·FeBr$_4$ and much larger θ values in **2**·FeCl$_4$ and **2**·FeBr$_4$. Nevertheless, it is difficult to explain the marked difference in θ between **2**·FeCl$_4$ and **2**·FeBr$_4$, and also the remarkably large θ value in **2**·FeBr$_4$, if it were not taken into account that the **2** molecule in **2**·FeBr$_4$ works as a better spin coupler than that in **2**·FeCl$_4$. This assumption is very likely, since the former salt possesses more mobile (conducting) π electrons than the latter salt, as is obvious from the comparison between their room-temperature electrical conductivities (7.0×10^{-2} and 1.8×10^{-4} S cm^{-1}). Moreover, if the conducting electrons move on the whole of the **2** column, the spin interaction in the longer Cl (or Br)···Cl (or Br) contact will also become important.

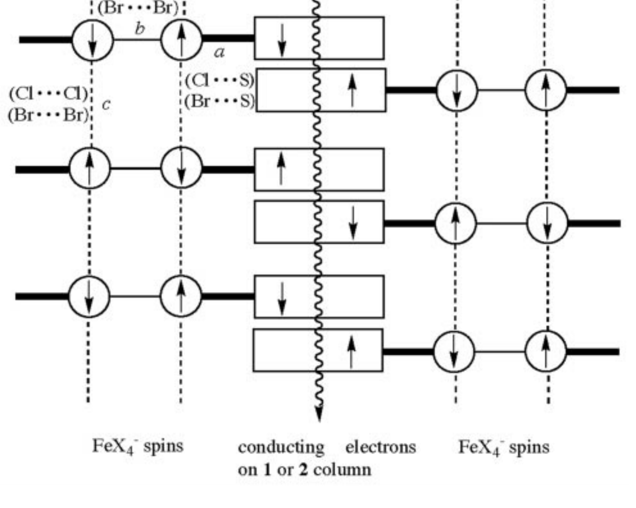

Fig. 6 Schematic spin arrangement in **1**·FeBr$_4$, **2**·FeCl$_4$ and **2**·FeBr$_4$.

Conclusions

Only the 1 : 1 charge-transfer salts of **1** and **2** with a magnetic FeCl$_4$ or FeBr$_4$ counteranion were obtained, contrary to our expectation of the corresponding 1 : 2 salts. As supposed from the 1 : 1 stoichiometry of the **1** or **2** molecule and FeCl$_4$ or FeBr$_4$ ion as well as from the strong dimerization of the two neighboring donor molecules within each one-dimensional **1** or **2** stacking column, the room-temperature electrical conductivities were low (7×10^{-2} S cm^{-1} maximum), which are however somewhat higher than those (10^{-6}–10^{-7} S cm^{-1}) in 1 : 1 FeCl$_4$ or FeBr$_4$ salts of BEDT-TTF and C$_1$TET-TTF. On the other hand, the interaction between the Fe(III) d spins on the FeCl$_4$ or FeBr$_4$ ions markedly changed between the three salts, as can be seen from their Weiss temperatures. In particular, the Weiss temperature of **2**·FeBr$_4$ was −31.2 K, which is the highest for the FeCl$_4$ or FeBr$_4$ salts known so far. This unusually strong spin interaction between the Fe(III) d spins can be reasonably regarded as an indirect one by aid of mobile (conducting) π electrons on the **2**-stacked column, based on the comparison between the crystal structures of the three salts. Through the present investigation it became clear that mobile π electrons work as a good spin coupler for the interaction between the d spins and also the degree of mobility has a great influence on the strength of spin interaction.

Acknowledgements

This work was supported by a Grant-in-Aid for Scientific Research on Priority Areas (B) (No. 11224209) from the Ministry of Education, Science and Culture, Japan.

References

1 P. Day, *Philos. Trans. R. Soc. London, Ser. A*, 1985, **314**, 145.
2 M. Kurmoo, A. W. Graham, P. Day, S. J. Coles, M. B. Hursthouse, J. L. Caulfield, J. Singleton, F. L. Pratt, W. Hayes, L. Ducasse and P. Guionneau, *J. Am. Chem. Soc.*, 1995, **117**, 12209.
3 E. Ojima, H. Fujiwara, K. Kato, H. Kobayashi, H. Tanaka, A. Kobayashi, M. Tokumoto and P. Cassoux, *J. Am. Chem. Soc.*, 1999, **121**, 5581.
4 E. Coronado, J. R. Galan-Mascaros, C. J. Gomez-Garcia and V. Laukhin, *Nature*, 2000, **408**, 447.
5 M. Iwamatsu, T. Kominami, K. Ueda, T. Sugimoto, H. Fujita and T. Adachi, *Chem. Lett.*, 1999, 329.
6 M. Iwamatsu, T. Kominami, K. Ueda, T. Sugimoto, T. Adachi, H. Fujita, H. Yoshino, Y. Mizuno, K. Murata and M. Shiro, *Inorg. Chem.*, 2000, **39**, 3810.
7 M. Iwamatsu, T. Kominami, K. Ueda, T. Sugimoto, T. Tada, K.-i. Nishimura, T. Adachi, H. Fujita, F. Guo, S. Yokogawa, H. Yoshino, K. Murata and M. Shiro, *J. Mater. Chem.*, 2001, **11**, 385.

8 T. Mallah, C. Hollis, S. Bott, M. Kurmoo, P. Day, M. Allan and R. H. Friend, *J. Chem. Soc., Dalton Trans.*, 1990, 859.

9 M. Kurmoo, P. Day, P. Guionneau, G. Bravic, D. Chasseau, L. Ducasse, M. L. Allan, I. D. Marsden and R. H. Friend, *Inorg. Chem.*, 1996, **35**, 4719.

10 T. Enoki, M. Enomoto, M. Enomoto, K. Yamaguchi, N. Yoneyama, J. Yamaura, A. Miyazaki and G. Saito, *Mol. Cryst. Liq. Cryst.*, 1996, **285**, 19.

11 A. Miyazaki, M. Enomoto, M. Enomoto, T. Enoki and G. Saito, *Mol. Cryst. Liq. Cryst.*, 1997, **305**, 425.

12 T. Enoki, T. Umeyama, A. Miyazaki, H. Nishikawa, I. Ikemoto and K. Kikuchi, *Phys. Rev. Lett.*, 1998, **81**, 3719.

13 H. Kobayashi, H. Tomita, T. Naito, A. Kobayashi, F. Sakai, T. Watanabe and P. Cassoux, *J. Am. Chem. Soc.*, 1996, **118**, 368.

14 A. Altomare, M. C. Burlea, M. Gamalli, M. Cascarano, C. Giacovazzo, A. Guagliardi and G. Polidre, *J. Appl. Crystallogr.*, 1994, **27**, 435.

15 P. T. Beurskens, G. Admiraal, G. Beurskens, W. P. Bosman, D. de Gelder, R. Israel and J. M. M. Smith, in *Technical Report of the Crystallography Laboratory*, University of Nijmegen, The Netherlands, 1994.

16 TeXsan, Crystal Structure Analysis Package, Molecular Structure Corporation, Houston, TX, 1985 & 1992.

17 E. König, *Landolt-Bornstein, Group II: Atomic and Molecular Physics, Vol. 2, Magnetic Properties of Coordination and Organometallic Transition Metal Compounds*, Springer-Verlag, Berlin, 1966.

18 L. Pauling, *The Nature of the Chemical Bond*, 3rd edn., Cornell University Press, Ithaca, New York, 1960.

19 M. Iwamatsu, T. Kominami, K. Ueda, T. Sugimoto and H. Fujita, unpublished results.